

**Supplemental information**

**Characteristic ERK1/2 signaling dynamics  
distinguishes necroptosis from apoptosis**

**François Sipieter, Benjamin Cappe, Aymeric Leray, Elke De Schutter, Jolien Bridelance, Paco Hulpiau, Guy Van Camp, Wim Declercq, Laurent Hélot, Pierre Vincent, Peter Vandenabeele, and Franck B. Riquet**

# Supplemental material

## Figure S1

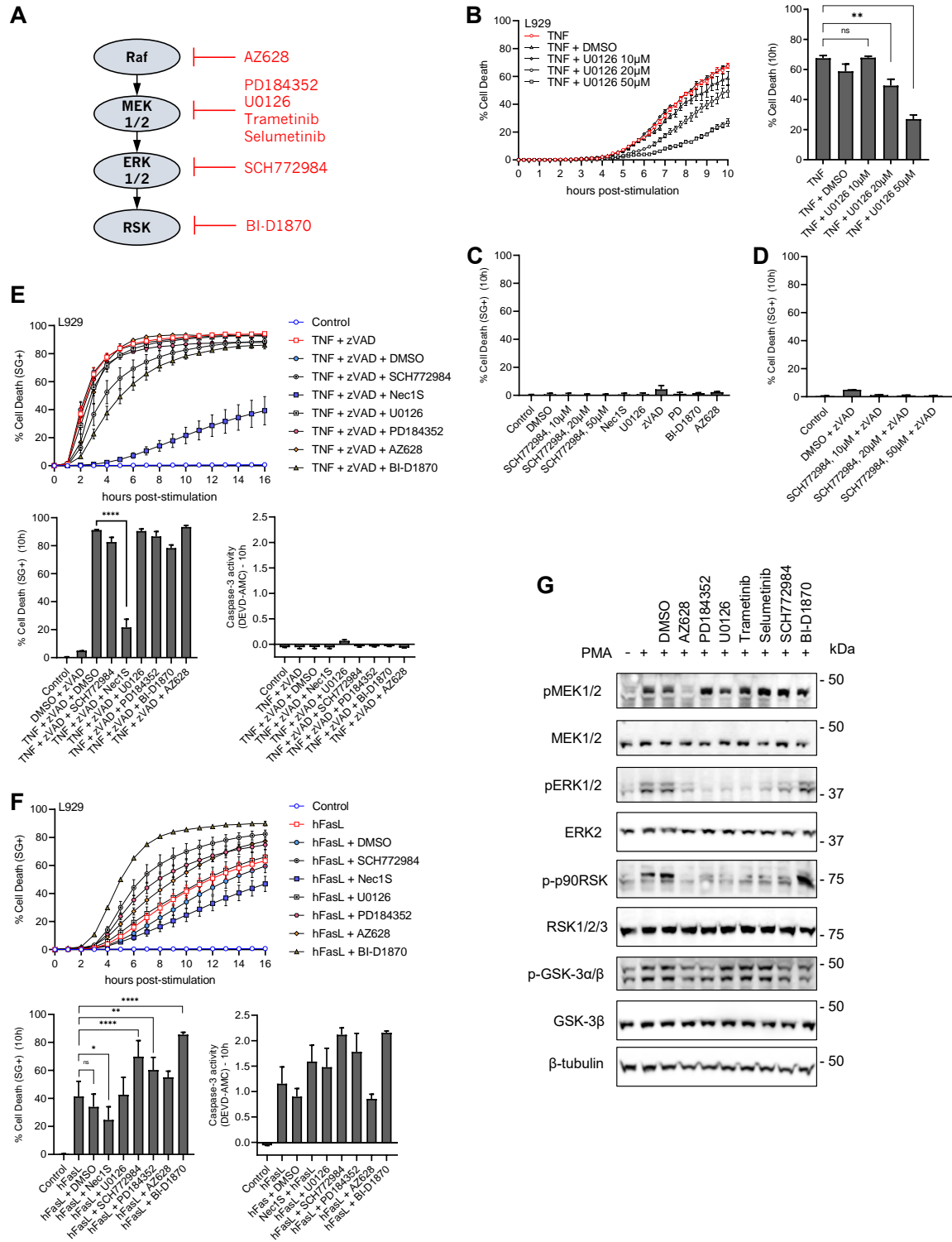
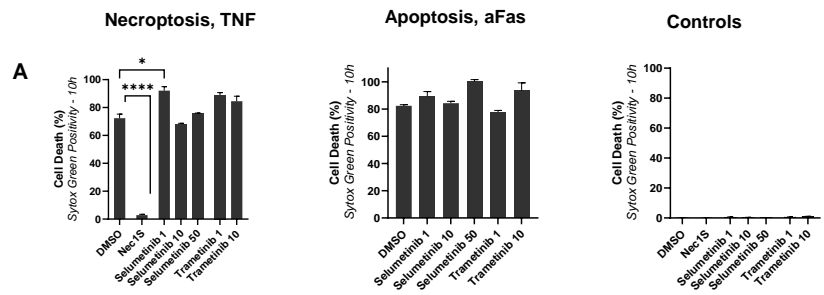


**Figure S1. Effect of MAPK/ERK1&2 signaling pathway inhibition in TNF-induced necroptosis and hFasL-induced apoptosis, related to Figure 1.**

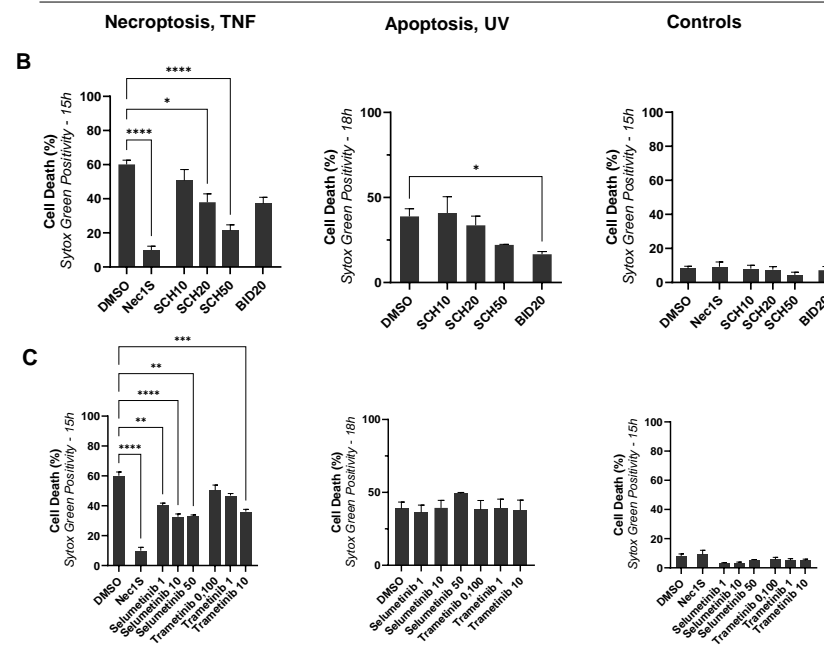
(A) Schematic overview of MAPK/ERK1&2 signaling pathway and corresponding inhibitors used in this study. (B) L929 wildtype cells were pretreated for 1 hour with U0126 in a dose-dependent manner or DMSO as a control before TNF (red) treatment. Cell death was quantified by the number of propidium positive over the total number of cells, measured as a function of time by video-microscopy (B, left panel), and plotted at 10 hours after TNF stimulation (B, right panel). (C and D) Cytotoxicity measurements (SG<sup>+</sup> positivity) in L929 wildtype cells 10 hours in the control condition. (E and F) L929 wildtype cells were pretreated for 1 hour with the indicated compounds targeting the MAPK/ERK1&2 pathway or RIPK1 activity before TNF+zVAD (E) or hFasL (F) treatment. Cell death was measured as a function of time by SytoxGreen (SG<sup>+</sup>) positivity (E-F, left graphs) and plotted at 10 hours after stimulation (E-F, middle graphs). Caspase-3 activity was assessed by DEVD-AMC cleavage efficiency (E-F, right graphs) 10 hours after stimulation. (G) L929 cells were stimulated or not with 500 nM PMA for 10 min and then treated for 10 min with the indicated MAPK/ERK pathway inhibitor or DMSO. Cells were then lysed and immunoblotted as indicated on the left of each blot. Data are presented as mean  $\pm$  SEM of at least two independent experiments. Statistical significance was determined using two-way ANOVA followed by a Tukey *post hoc* test. Significance between samples is indicated as follows: \* $P$  < 0.05; \*\* $P$  < 0.01; \*\*\* $P$  < 0.001; ns, not significant.

Figure S2

**L929sAhFas**



**Jurkat FADD<sup>-/-</sup>**



**HT-29**

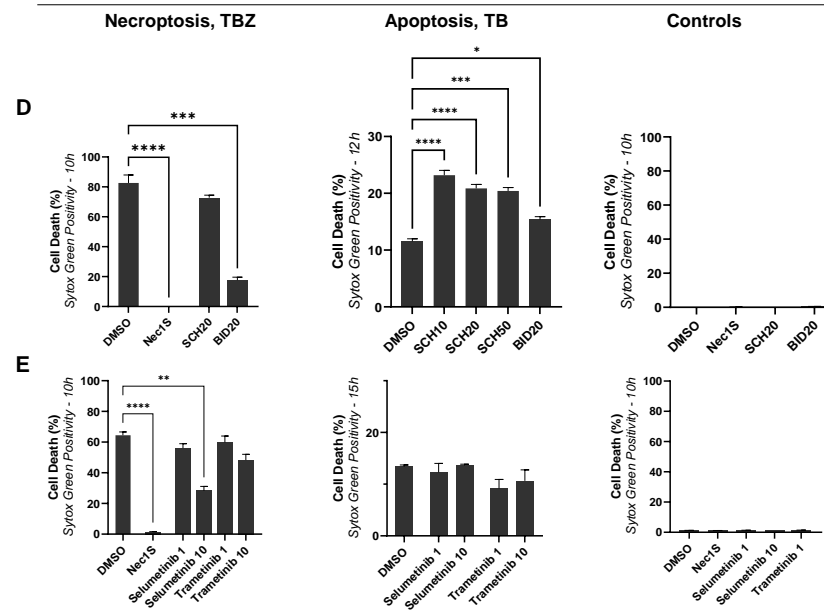


**Figure S2. Effect of advanced MEK1/2 inhibitors, ERK1/2, and RSK inhibitors on necroptosis and apoptosis in different cellular models, related to Figure 1.**

(A) Dose-dependent response of L929 wildtype cells pretreated for 1 hour with advanced MEK1/2 inhibitors (Selumetinib and Trametinib) or Nec1S before stimulation. (B-E) Jurkat FADD<sup>-/-</sup> (B-C) and HT29 (D-E) were pretreated 1 hour with different concentrations of SCH772984 or with BI-D1870 at 20  $\mu$ M (B and D) or with advanced MEK1/2 inhibitors (C and E) before stimulation. For each panel, cell death (necroptosis (left), apoptosis (center), or control (right)) was measured by SytoxGreen. TBZ: TNF+BV6+zVAD, TB: TNF+BV6. Data are presented as mean  $\pm$  SEM of at least two independent experiments. Statistical significance was determined using two-way ANOVA followed by a Tukey *post hoc* test. Significance between samples is indicated as follows: \* $P < 0.05$ ; \*\* $P < 0.01$ ; \*\*\* $P < 0.001$ .

**Figure S3**

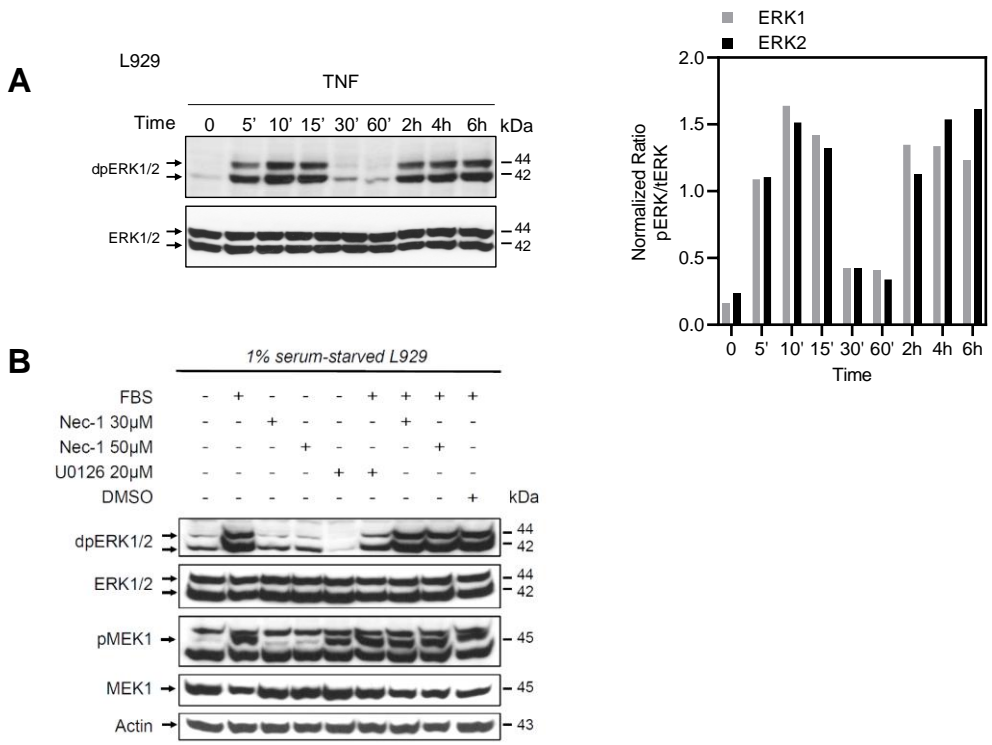


**Figure S3. RIPK1 activity inhibition does not prevent serum-stimulated MEK1/2 and ERK1/2 activation, related to Figure 2.**

(A) L929 cells were serum-deprived (1% fetal calf serum: FCS) for 12 h and then stimulated with TNF for the indicated time points. Cells were then lysed and immunoblotted as indicated on the left of each blot. Histogram of densitometry analysis of phospho-ERK/total ERK1/2 level at each time point is presented both for ERK1 and ERK2 signal. (B) L929 cells were serum-deprived (1% FCS) for 12h and then pretreated for 30 min with either Nec1S at 30  $\mu$ M and 50  $\mu$ M or U0126 at 20  $\mu$ M, or DMSO (volume equivalent to 50  $\mu$ M treatment condition) before being growth factor-stimulated (10% FCS). Cells were then lysed and immunoblotted as indicated on the left of each blot.

Figure S4

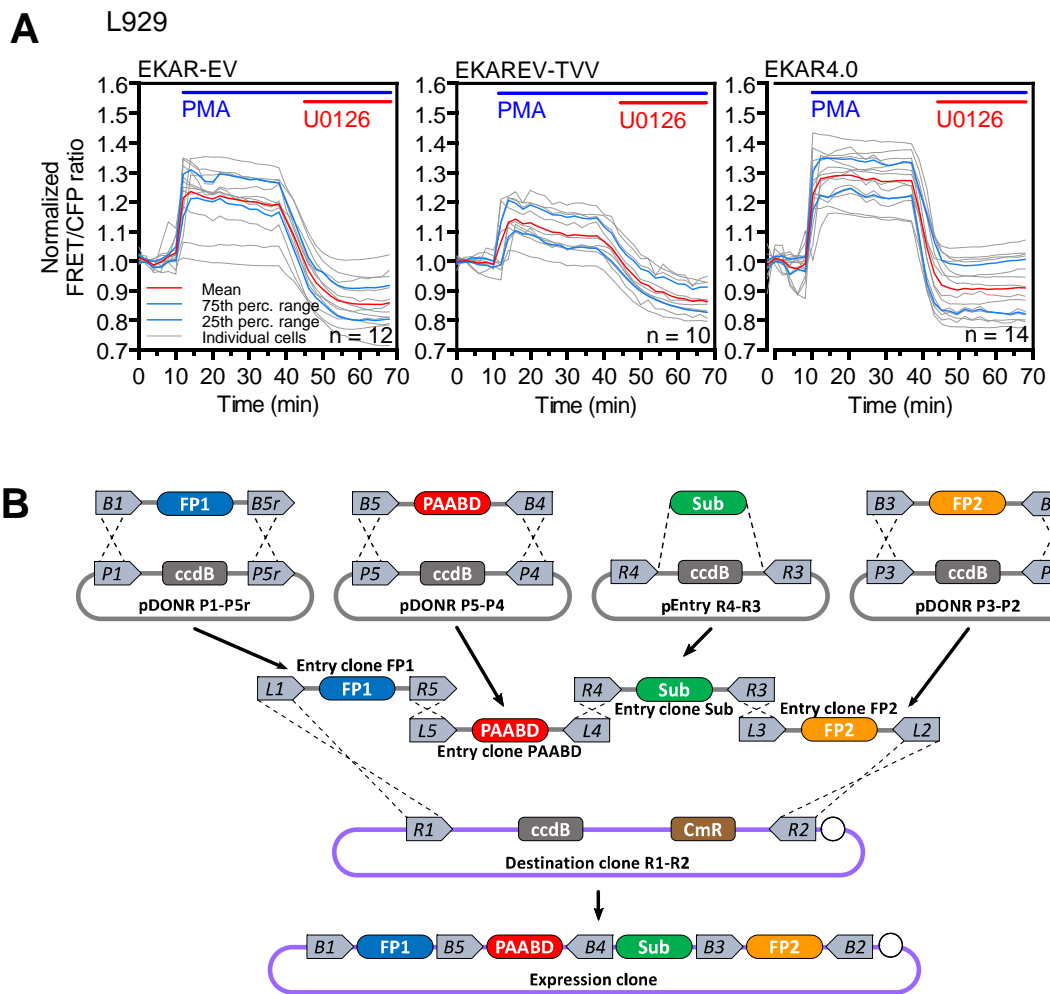




**Figure S4. Strategy for versatile generation of genetically encoded FRET biosensors using multisite Gateway cloning, related to Figure 3.**

(A) Biosensor reference experiments: L929 cells expressing EKAR-EV (left), EKAR-EV-TVV (middle), and EKAR4.0 (right) were time lapse-imaged by FRET microscopy and treated with PMA (0,5  $\mu$ M) at  $t= 10$  min and then with U0126 (20  $\mu$ M) at  $t= 40$  min. Graphs present FRET/CFP ratio values of every single cell normalized to the averaged baseline FRET/CFP ratio value throughout reference experiments. FRET biosensor data are displayed in two ways: all individual cell responses (grey curves), the population mean in red, and the 25<sup>th</sup> and 75<sup>th</sup> percentile values in blue. Cells were imaged at the rate of 1 acquisition every 2 minutes for a total duration of 70 minutes. Cell number (n) is reported on each graph. (B) Schematic representation of the cloning strategy based on multisite gateway for the generation of entry vectors of the library containing one functional element of a FRET biosensor (Nt or Ct terminally tagging fluorescent protein (FP1/FP2), phospho-amino acid-binding domain (PAABD), and a specific substrate for the kinase of interest (Sub), and the multisite Gateway recombination att sites. The insertion of *attB1*, *attB5*, *attB4*, *attB3*, and *attB2* recombination sites connects each functional domain of the resulting FRET biosensor acting as linkers. The detailed cloning strategy can be found in the *Materials & Methods* section.

Figure S5

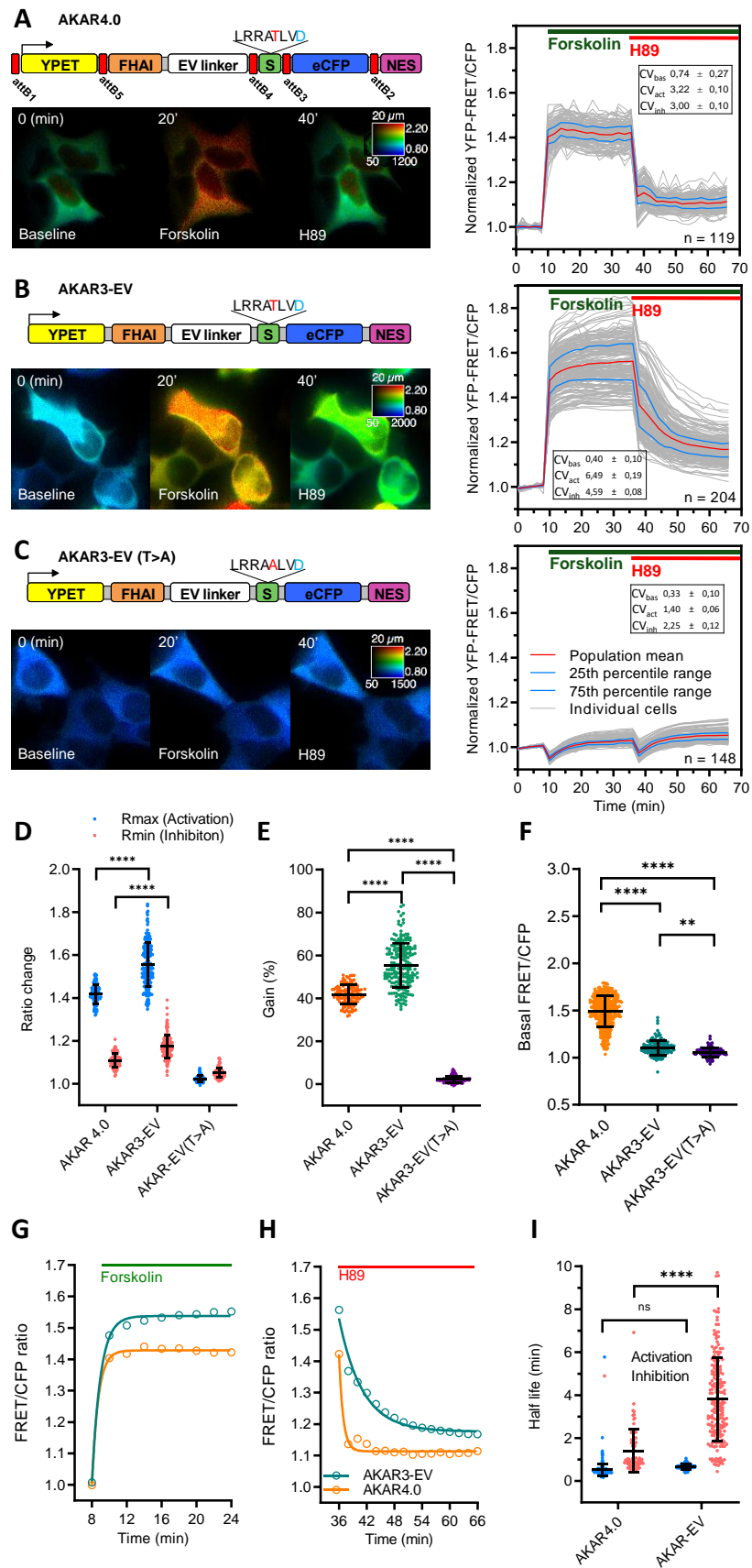


**Figure S5. Multisite Gateway cloning improves the reversibility of AKAR3-EV, related to Figure 3.**

(A-C) Biosensor reference experiments: HEK cells expressing AKAR3-EV GW4.0 (A), AKAR3-EV (B) or its mutant version, AKAR3-EV (T>A) (C) were time lapse-imaged by FRET microscopy and treated with Forskolin (12.5  $\mu$ M) at  $t= 10$ min and then with H89 (10  $\mu$ M) at  $t= 34$  min. Top of each panel: Schematic representation of PKA Kinase Activity Reporter (AKAR) construct used. The small red rectangles in (A) map the positions of obligated *attB* linkers between each FRET biosensor domain. For the substrate peptide sequence, red letters indicate the phosphorylation site, and blue letters indicate amino-acid substitutions to increase the affinity for the WW domain, Bottom left of each panel: Pseudo-color FRET/CFP ratio images of PKA activity at the steady-state ( $t= 0$  min), upon Forskolin ( $t= 20$  min) and H89 treatment ( $t= 40$  min). Right of each panel: Graph presenting the FRET/CFP ratio values of every single cell normalized to the averaged baseline FRET/CFP ratio value throughout reference experiments. All individual cells (grey curves), as well as the mean (red curve) and the 25th and 75th percentile range (blue curves) from at least 100 cells, are plotted as a function of time.  $CV_{bas}$ ,  $CV_{act}$ , and  $CV_{inh}$  indicate the coefficient of variation for cells at the baseline, cells in PKA activated state, and cells in the PKA inhibited state, respectively. Imaging parameters were kept identical for the different biosensors tested. Cells were imaged for a total duration of 70 minutes at the rate of 1 acquisition every 2 minutes. (D-I) Characterization and comparison of different AKAR FRET biosensors responses were performed based on the following parameters: ratio changes ( $R_{min}$ ,  $R_{max}$ ) (D), gain (E), basal FRET /CFP value without any stimulation (F), and fitted curves to determine the speed of activation upon PKA activation (G, I) and the reversibility of the biosensor upon PKA inhibition (H, I). Fitted curves were plotted based on  $\tau_{1/2}$ , which is the time value representing half of the measured duration of the inhibition or activation phase.  $\tau_{1/2}$  was calculated by applying a non-linear regression curve on ration values over the complete set of individual cells during the activation or inhibition phase. Nonlinear regression was calculated between  $t= 8$  min and  $t= 24$  min for the activation, and between  $t= 36$  min and  $t= 66$  min for the inhibition, and plotted as a fitted curved. All calculations were performed using GraphPad PRISM 8. Data are mean  $\pm$  SD from at least two independent experiments. Scale bar: 10  $\mu$ m. The number of cells analyzed is indicated by n (A-C). Statistical significance was determined using two-way ANOVA followed by a Tukey *post hoc* test. Significance between samples is indicated as follows: \* $P < 0.05$ ; \*\* $P < 0.01$ ; \*\*\* $P < 0.001$ ; ns, not significant.

**Figure S6**

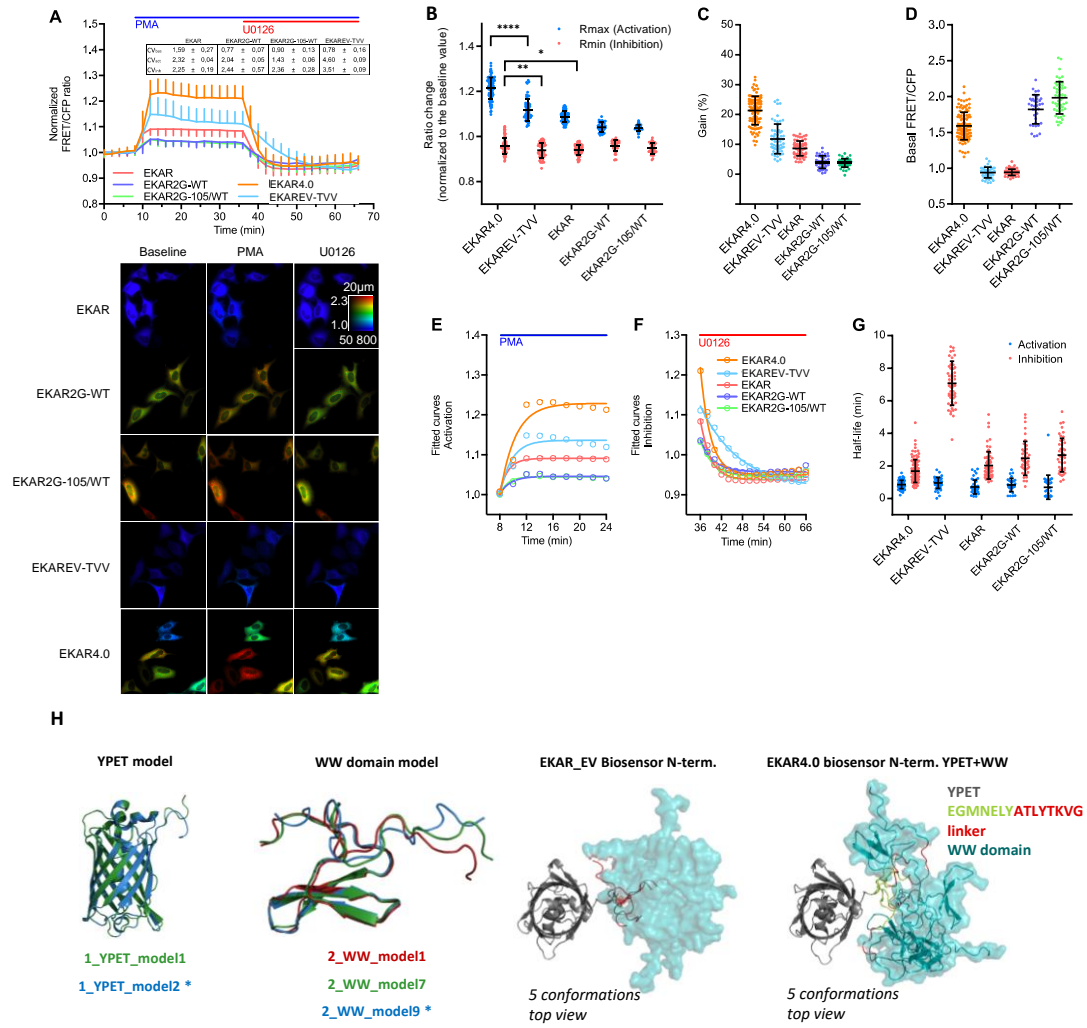


**Figure S6. Comparison of EKAR4.0 to previous EKAR biosensors, related to Figure 3.**

(A) Biosensor reference experiments: HeLa cells expressing EKAR, EKAR-EV, EKAR-EV-TVV, EKAR2G-WT, and EKAR2G-105/WT were time lapse-imaged by FRET microscopy and treated with PMA (0.5  $\mu$ M) at  $t= 10$  min and then with U0126 (20 $\mu$ M) at  $t= 34$  min. Upper panel: graph presenting the FRET/CFP ratio values of every single cell normalized to the averaged baseline FRET/CFP ratio value throughout reference experiments. Data are presented as mean  $\pm$  SD from at least two independent experiments, and at least 40 cells are plotted as a function of time.  $CV_{bas}$ ,  $CV_{act}$ , and  $CV_{inh}$  indicate the coefficient of variation for cells at the baseline, cells in ERK1/2 activated state, and cells in the ERK1/2 inhibited state, respectively. Imaging parameters were kept identical for the different biosensors tested. Cells were imaged for a total duration of 70 minutes at the rate of 1 acquisition every 2 minutes. Pseudo-color FRET/CFP ratio images of ERK1/2 activity at the steady-state ( $t= 0$  min), upon PMA addition ( $t= 20$  min) and U0126 addition ( $t= 40$  min) are shown. Scale bar: 20  $\mu$ m. (B-G) Characterization and comparison of all ERK1/2 biosensors responses were performed based on the following parameters: ratio changes ( $R_{min}$ ,  $R_{max}$ ) (B), gain (C), basal FRET /CFP value without any stimulation (D), and fitted curves to determine the speed of activation upon ERK1/2 activation (E and G) and the reversibility of the biosensor upon MEK1/2 inhibition (F and G). Fitted curves were plotted based on  $\tau_{1/2}$ , which is the time value representing half of the measured duration of the inhibition or activation phase.  $\tau_{1/2}$  was calculated by applying a non-linear regression curve on ration values over the complete set of individual cells during the activation or inhibition phase. The nonlinear regression was calculated between  $t= 8$  min and  $t= 24$  min for the activation and between  $t= 36$  min and  $t= 66$  min for the inhibition and plotted as fitted curves. All calculations were performed using GraphPad PRISM 8. (H) Predicted 3D models of YPET, WW domain, and N-terminal of ERK1/2 biosensors with (EKAR4.0) and without (EKAR\_EV) *att* linkers. Green letters correspond to residues from *att* linker within the Eevee linker in red letters. The sampling of their conformational spaces is indicated below each 3D model.

**Figure S7**

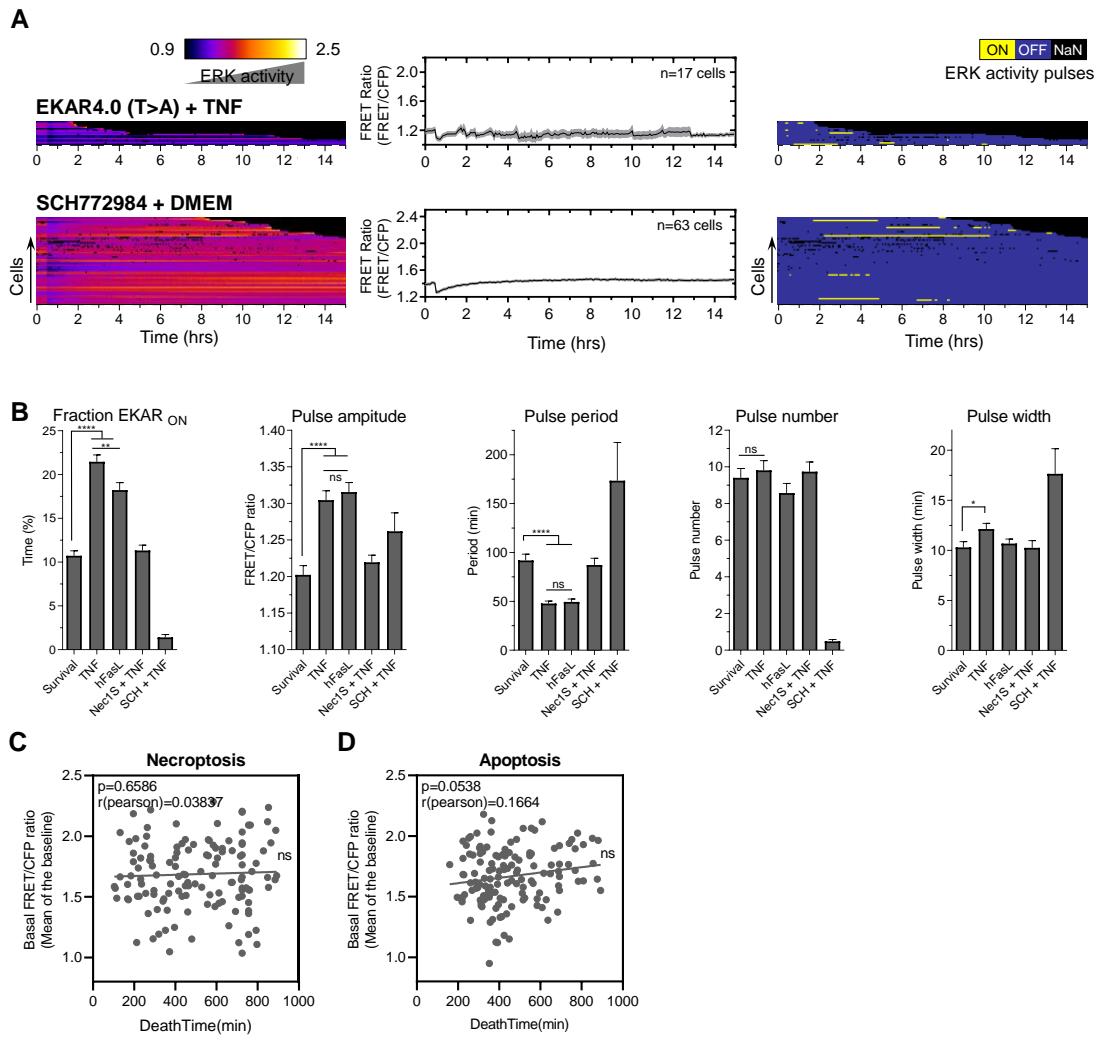


**Figure S7. Basal ERK1/2 activity does not correlate with cellular death time, related to Figure 4 & 5.**

(A) Biosensing experiment: L929 expressing the negative control FRET biosensor EKAR-EV-TA GW4.0 (upper panel) or EKAR4.0 (bottom panel) were treated with TNF or DMEM as internal controls, respectively. From left to right, results are displayed as follows: FRET/CFP ratio of every single cell displayed by a FRET/CFP ratio kymographic representation (left), averaged FRET/CFP ratio (mean±SEM) as a function of time (middle), the corresponding pattern of ERK1/2 pulse dynamics displayed by a binary kymographic representation of ERK<sub>ON</sub> and ERK<sub>OFF</sub> states (right). Experimental and analysis protocols, as well as graphical representations, are the same as in Fig 4 and 5. (B) Global quantitative analysis of EKAR4.0 pulse dynamics from data presented in Fig 5 were calculated from 1h after the start of imaging until the end of the experiment, for each cell and each condition described in Fig 4. This global data analysis is presented as histograms. It corresponds to the mean±SEM of at least two independent experiments for the following parameters, from left to right: EKAR<sub>ON</sub> state (calculated for each cell, normalized to the cell life duration of each cell, and expressed in percentage of time of the cell lifespan), pulse amplitude, pulse period (min), pulse number measured during the entire experiment, pulse width (min). Statistical significance was determined using two-way ANOVA followed by a Tukey *post hoc* test. Significance between samples is indicated as follows: \* $p < 0.05$ ; \*\* $p < 0.01$ ; \*\*\* $p < 0.001$ ; \*\*\*\* $p < 0.0001$ ; *ns*, not significant. (C-D) From experimental data presented in Fig 4, a scatterplot of single-cell measurements of basal ERK1/2 activity plotted against the time of cell death induced by TNF (C) or hFasL (D) stimulation. The dark line indicates a linear fit, and the corresponding *p* values are indicated. A Pearson's correlation was performed to assess the linear relationship between variables.

**Figure S8**

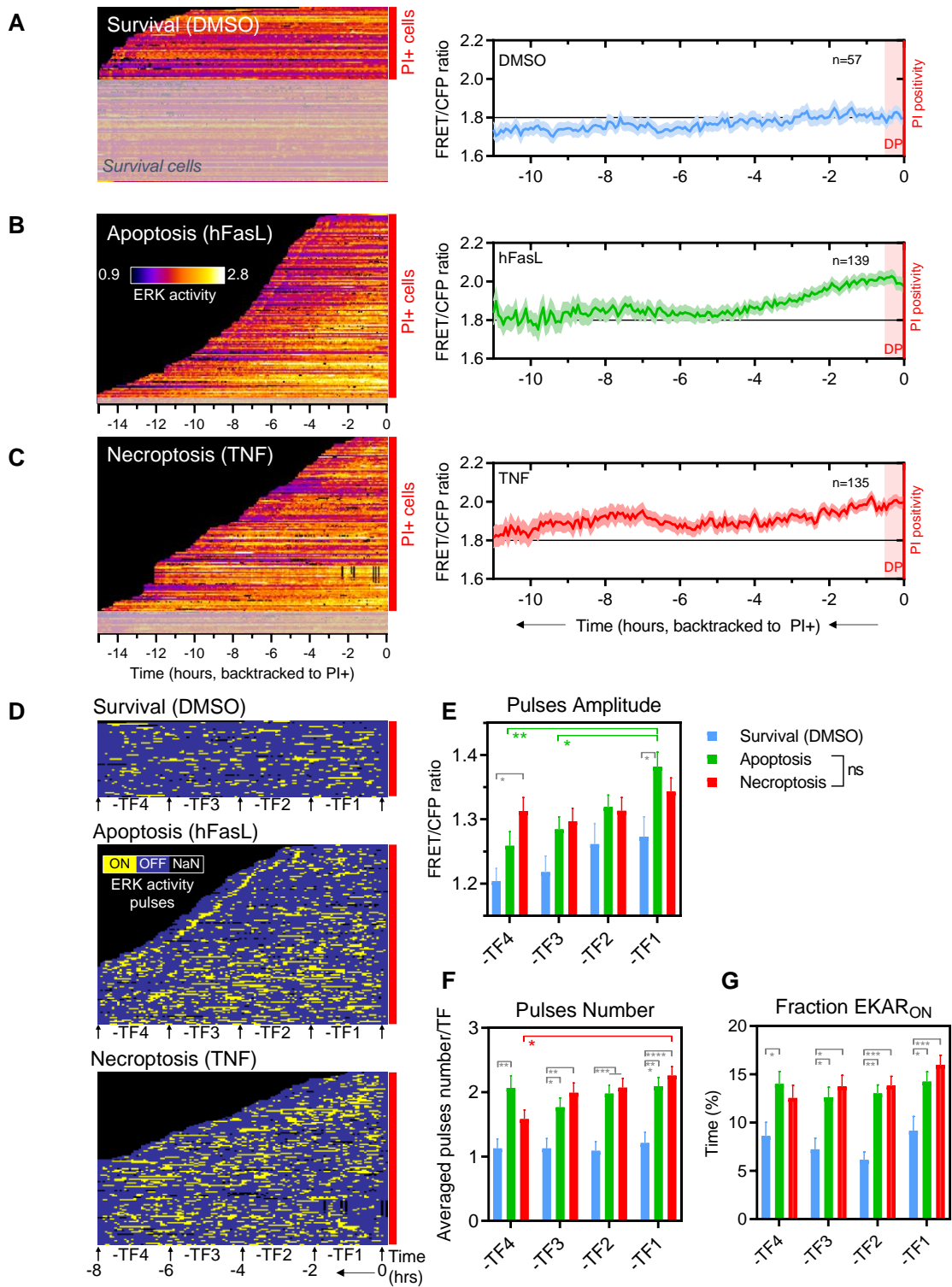




**Figure S8. Time-resolved analysis of ERK1/2 activity dynamics preceding death events distinguishes necroptosis from apoptosis, related to Figure 4 & 5.**

(A-C) From experimental data presented in Fig 4, dead cells identified using propidium iodide staining were systematically backtracked in three cellular contexts (survival (A), apoptosis (B), necroptosis (C)). The FRET/CFP ratio is displayed using a kymographic representation (left panels) and is then averaged (mean  $\pm$  SEM) and plotted as a function of time, starting at the moment of cell death (red lines, PI+) (right panels). The light red area preceding cell death (30 minutes) corresponds to the disintegration phase (DP). The number of cells analyzed is reported on each graph (n). (D) The associated binary kymographs for ERK1/2 pulses detection are shown for each experimental condition. (E-F) Time-resolved quantitative analysis of EKAR4.0 signal in single cells was performed. Data are presented as histograms of ERK1/2 pulses amplitude (E) and ERK1/2 pulses number (F), when stimulated or not (control) with hFasL (apoptosis) or TNF (necroptosis). These parameters were calculated just after the time window corresponding to the DP (30 min) with a 2-hours-backtracked time interval for each cell and each condition (TF: Temporal frame). Statistical significance was determined using two-way ANOVA followed by a Tukey post hoc test. Significance between samples is indicated as follows: \* $p < 0.05$ ; \*\* $p < 0.01$ ; \*\*\* $p < 0.001$ ; \*\*\*\* $p < 0.0001$ ; ns, not significant.

Figure S9

A

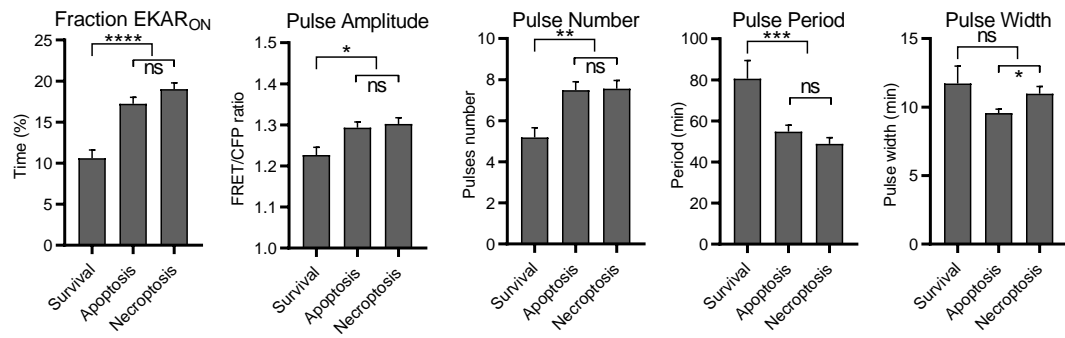


**Figure S9. Metrics from global analysis of ERK1/2 activity dynamics preceding death events, related to Figure 4 & 5.**

(A) Similarly to Fig S7B, global quantitative analysis of EKAR4.0 signal from data presented in Fig S8D was calculated just after the time window corresponding to the DP (30 minutes before PI positivity) until the end of TF4 (corresponding to 8 hours backtracked time interval), for each cell and each condition.

**Figure S10**

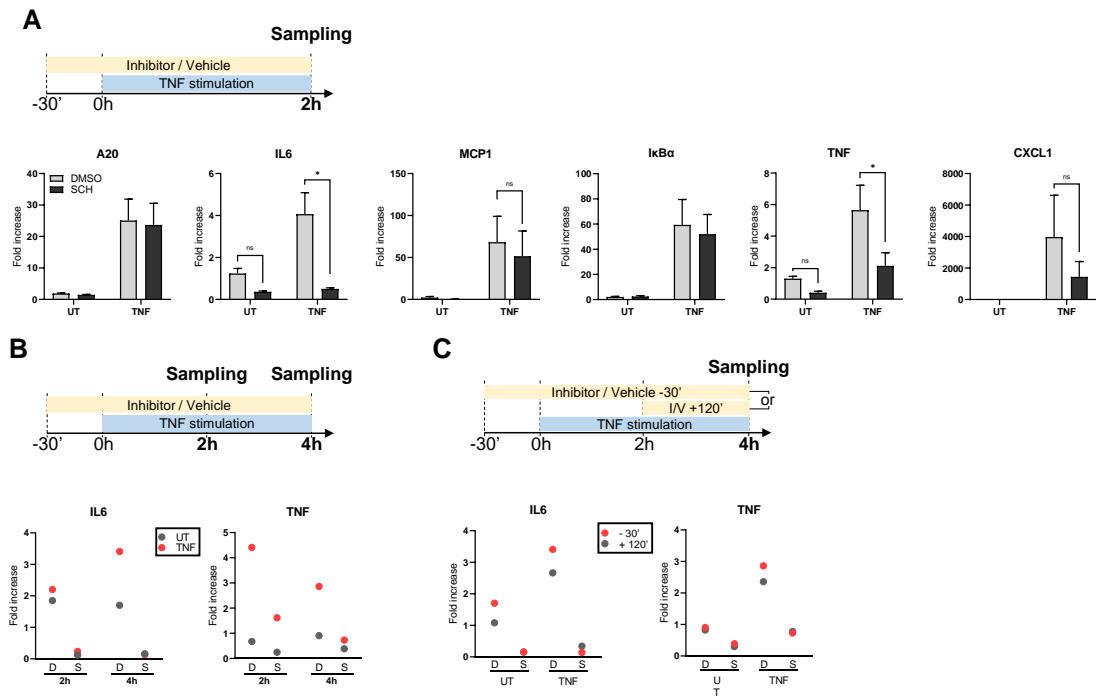


**Figure S10. Direct ERK1/2 inhibition before or after TNF treatment impairs inflammatory genes expression profiles in L929 during necroptosis, related to Figure 4, 5 & 6.**

(A-B) L929 cells were pretreated with 10  $\mu$ M SCH772984 or vehicle control for 30 minutes and then stimulated or not with TNF for 2 hours (A) or 2 and 4 hours (B). Cells were then harvested and processed for RT-qPCR reactions. Key cytokines, chemokines gene products were tested at 2 hours post-induction. Only the ones showing differences at this time point were further studied at two different time points (2 and 4 hours post-stimulation). (C) L929 cells were treated with TNF for 4 hours. ERK1/2 inhibitor SCH772984 (10  $\mu$ M) or vehicle control was added 30 min before or 2 hours after TNF stimulation. All data are presented as mean $\pm$ SEM of two independent experiments (A) and a single experiment (B and C). Statistical significance was determined using an unpaired t-test between DMSO and SCH. Significance between samples is indicated as follows: \* $p$  < 0.05; \*\* $p$  < 0.01; \*\*\* $p$  < 0.001; *ns*, not significant. SCH, SCH772984, UT, untreated,

**Figure S11**

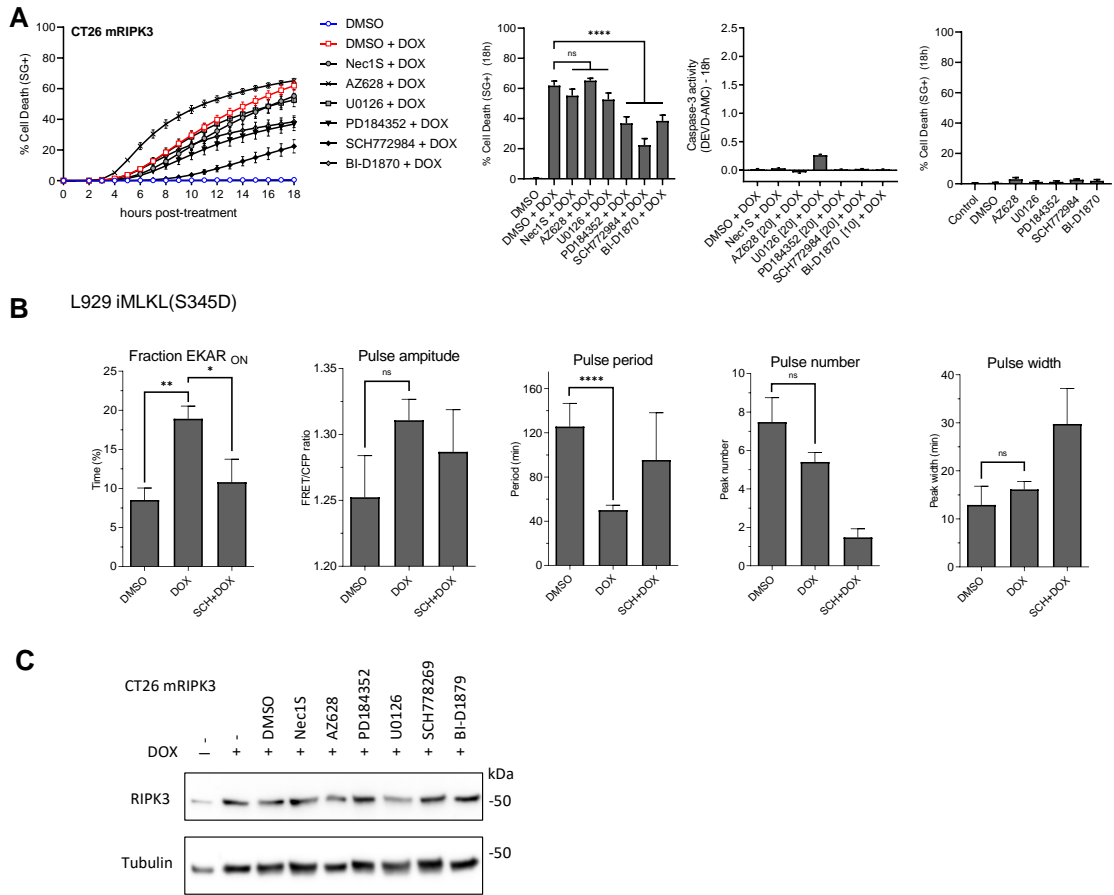


**Figure S11. Inhibition of the MAPK/ERK1&2 pathway downstream of MEK1/2 efficiently impairs necroptosis induced by RIPK3 overexpression, related to Figure 7.**

(A) RIPK3-deficient CT26 cells reconstituted with inducible wildtype RIPK3 were pretreated for 1 hour with the indicated compounds before Dox (red) or DMEM (blue) treatment (grey curves). Cell death was measured as a function of time by SytoxGreen (SG<sup>+</sup>) positivity (kinetic experiment, left), 18 hours after Dox stimulation (A, left histogram), and caspase-3 activity was assessed by DEVD-AMC cleavage efficiency (A, middle histogram) 18 hours after Dox stimulation. Drugs-induced toxicity measurements (SG<sup>+</sup> positivity) 18 hours after DMEM stimulation (A, right histogram). All cell death data are presented as mean±SEM of at least four independent experiments. Statistical significance was determined using two-way ANOVA followed by a Tukey *post hoc* test. Significance between samples is indicated as follows: \**p* < 0.05; \*\**p* < 0.01; \*\*\**p* < 0.001; *ns*, not significant. (B) Global quantitative analysis of EKAR4.0 pulse dynamics in L929 iMLKL (S345D) from Figure 7 were calculated from 1h after the start of imaging until the rest of the experiment for each cell. This global data analysis is presented as histograms like in Figure S6B and corresponds to the mean±SEM of at least two independent experiments. Statistical significance was determined using two-way ANOVA followed by a Tukey *post hoc* test. Significance between samples is indicated as follows: \**p* < 0.05; \*\**p* < 0.01; \*\*\**p* < 0.001; \*\*\*\**p* < 0.0001; *ns*, not significant. (C) CT26 mRIPK3 cells were pretreated or not for 1 hour with the indicated compounds and subsequently stimulated with Dox. Cells were then lysed and immunoblotted as indicated on the left of each blot. Corresponding molecular weights are reported on the right of each blot.

**Table S1. Protein sequences comparison between EKAR-EV and EKAR4.0, related to Figure 3.**

<b>EKAR-EV</b>
<b>YPET</b>
MVSKGEELFTGVVPIIIVELDGDVNGHKFSVSGEGEGDATYGKLTLLKLLCTTGKLPVPWPPTLVTTTLGYGLQCFARYPDHMKQHDFFKSA MPEGYVQERTIFFKDDGNYKTRAEVKFEGDTLVNRIELKGIDFKEDGNILGHKLEYNYNSHNVIITADKQKNGIKANFKIRHNIEDGG VQLADHYQQNTPIGDGPVLLPDNHLYSYQSALFKDPNEKRDHMLLEFLTAAGITEGMNELY
<b>Linker</b>
LE
<b>WW Domain</b>
MADEEKLPFGWEKRMSRSSGRVYYFNHITNASQWERPSGNSSSGKNGQGE PAR
<b>EV linker</b>
GTSAGGSAGGSAGGSAGGSAGGSGSAGGSAGGSTSAGGSAGGSAGGSAGGSAGGSGSAGGSAGGSTSAGGSAGGSAGGSAGGSAGGSG SAGGSAGGSTSAGGSAGGSAGGSAGGSAGGSG
<b>Substrate + Docking site</b>
PDVPRTPVDKAKLSFQFP
<b>Linker</b>
GGR
<b>eCFP</b>
MVSKGEELFTGVVPIIIVELDGDVNGHKFSVSGEGEGDATYGKLTLLKFICTTGKLPVPWPPTLVTTTLTWGVQCFSRYPDHMKQHDFFKSA MPEGYVQERTIFFKDDGNYKTRAEVKFEGDTLVNRIELKGIDFKEDGNILGHKLEYNYISHNVIITADKQKNGIKANFKIRHNIEDGS VQLADHYQQNTPIGDGPVLLPDNHLYSTQSALS KDPNEKRDHMLLEFVTAAGITLGMDELYK
<b>EKAR4.0</b>
<b>YPET</b>
MVSKGEELFTGVVPIIIVELDGDVNGHKFSVSGEGEGDATYGKLTLLKLLCTTGKLPVPWPPTLVTTTLGYGLQCFARYPDHMKQHDFFKSA MPEGYVQERTIFFKDDGNYKTRAEVKFEGDTLVNRIELKGIDFKEDGNILGHKLEYNYNSHNVIITADKQKNGIKANFKIRHNIEDGG VQLADHYQQNTPIGDGPVLLPDNHLYSYQSALFKDPNEKRDHMLLEFLTAAGITEGMNELY
<b>Linker</b>
ATLYTKVG
<b>WW Domain</b>
MADEEKLPFGWEKRMSRSSGRVYYFNHITNASQWERPSGNSSSGKNGQGE PAR
<b>EV linker</b>
GTSAGGSAGGSAGGSAGGSAGGSGSAGGSAGGSTSAGGSAGGSAGGSAGGSAGGSGSAGGSAGGSTSAGGSAGGSAGGSAGGSAGGSG SAGGSAGGSTSAGGSAGGSAGGSAGGSAGGSG
<b>Linker</b>
NPTFLYKVGPG
<b>Substrate + Docking site</b>
PDVPRTPVDKAKLSFQFP
<b>Linker</b>
LEATLYNKVG
<b>eCFP</b>
MVSKGEELFTGVVPIIIVELDGDVNGHKFSVSGEGEGDATYGKLTLLKFICTTGKLPVPWPPTLVTTTLTWGVQCFSRYPDHMKQHDFFKSA MPEGYVQERTIFFKDDGNYKTRAEVKFEGDTLVNRIELKGIDFKEDGNILGHKLEYNYISHNVIITADKQKNGIKANFKIRHNIEDGS VQLADHYQQNTPIGDGPVLLPDNHLYSTQSALS KDPNEKRDHMLLEFVTAAGITLGMDELYK



**Table S2. Primers used for assessing pro-inflammatory cytokines expression levels by Q-PCR, related to Figure S10.**

<i>Mouse Gene</i>	<i>Forward primer</i>	<i>Reverse primer</i>
<i>Il-6</i>	TTCTCTGGGAAATCGTGGAAA	TCAGAATTGCCATTGCACAAC
<i>Mcp1</i>	GCATCTGCCCTAAGGTCTTCA	TGCTTGAGGTGGTTGTGGAA
<i>IκB-α</i>	ACGAGGAGTACGAGCAAATGGTG	TGATTGCCAAGTGCAGGAACGAG
<i>A20</i>	AGCACCCCTTAAGGAGACAGACAC	TCCCATTTCGTCATTCCAGTTCCG
<i>TNF-α</i>	ACCCTGGTATGAGCCCATATAC	ACACCCATTCCCTTCACAGAG
<i>Cxcl1</i>	CTATCGCCAATGAGCTGCG	TCTGAACCAAGGGAGCTTCA